

1 **SUPPLEMENTARY MATERIALS: RANDOMIZED SUB-SAMPLED**
2 **METHODS FOR MATRIX APPROXIMATION**

3 ANDREW AZZAM*, BENJAMIN ONG†, AND ALLAN STRUTHERS‡

4 **SM1. Additional Non-Accelerated Computational Results.** The conver-
5 gence test from [subsection 4.1](#) was performed on the remaining matrices tested in
6 [\[SM3\]](#). As before, these figures show: BFGS(\diamond) as specified by [Eq. \(2.5\)](#); DFP (\diamond)
7 as specified by [Eq. \(2.4\)](#); NS (\otimes) as specified by [Algorithm 2.1](#); SS1 (\bullet) as specified
8 by [Algorithm 2.2](#); SS2 (\blacksquare) as specified by [Algorithm 2.3](#). All numerical experiments
9 indicate that our non-accelerated sub-sampled algorithms converge predictably and
10 consistently,

- 11 • [Figure SM1](#) the LibSVM matrix AloI of size $n = 128$;
- 12 • [Figure SM2](#) the LibSVM matrix Protein of size $n = 357$;
- 13 • [Figure SM3](#) the LibSVM matrix Real-Sim of size $n = 20958$;
- 14 • [Figure SM4](#) the Sparse Suite matrix ND6K of size $n = 18000$;
- 15 • [Figure SM5](#) the Sparse Suite matrix ex9 of size $n = 3363$;
- 16 • [Figure SM6](#) the Sparse Suite matrix Chem97ZtZ of size $n = 2541$.
- 17 • [Figure SM7](#) the Sparse Suite matrix Body of size $n = 17556$.
- 18 • [Figure SM8](#) the Sparse Suite matrix bcstck of size $n = 11948$.
- 19 • [Figure SM9](#) the Sparse Suite matrix wathen of size $n = 30401$.

20 Plots in [Figures SM3, SM4, and SM7 to SM9](#) indicate that a maximum running time
21 is reached for the sub-sampled methods.

22 **SM2. Additional Accelerated Computational Results.** The convergence
23 test from [section 5](#) was performed on the remaining matrices tested in [\[SM3\]](#). We
24 illustrate the relative performance of the following algorithms:

- 25 • ($*$) BFGSA, [Eq. \(2.5\)](#) with adaptive sampling described in [\[SM3\]](#),
- 26 • (\circ) S1, [Eq. \(2.3\)](#) with $W = I_n$,
- 27 • (\triangleleft) SS1A+, [Algorithm 5.1](#)
- 28 • (\diamond) BFGS, [Eq. \(2.5\)](#),
- 29 • (\diamond) DFP, [Eq. \(2.4\)](#)

30 on the following matrices:

- 31 • [Figure SM10](#) the LibSVM matrix AloI of size $n = 128$;
- 32 • [Figure SM11](#) the LibSVM matrix Protein of size $n = 357$;
- 33 • [Figure SM12](#) the LibSVM matrix Real-Sim of size $n = 20958$;
- 34 • [Figure SM13](#) the Sparse Suite matrix ND6K of size $n = 18000$;
- 35 • [Figure SM14](#) the Sparse Suite matrix ex9 of size $n = 3363$;
- 36 • [Figure SM15](#) the Sparse Suite matrix Chem97ZtZ of size $n = 2541$.
- 37 • [Figure SM16](#) the Sparse Suite matrix Body of size $n = 17556$.
- 38 • [Figure SM17](#) the Sparse Suite matrix bcstck of size $n = 11948$.
- 39 • [Figure SM18](#) the Sparse Suite matrix wathen of size $n = 30401$.

40 The accelerated method [Algorithm 5.1](#) performs well on all matrices including those
41 with large $n \approx 10^4$ (see [Figures SM12, SM13, and SM16 to SM18](#)).

42 REFERENCES

*Department of Mathematical Sciences, Michigan Technological University (atazzam@mtu.edu).

†Department of Mathematical Sciences, Michigan Technological University (ongbw@mtu.edu).

‡Department of Mathematical Sciences, Michigan Technological University (struther@mtu.edu).

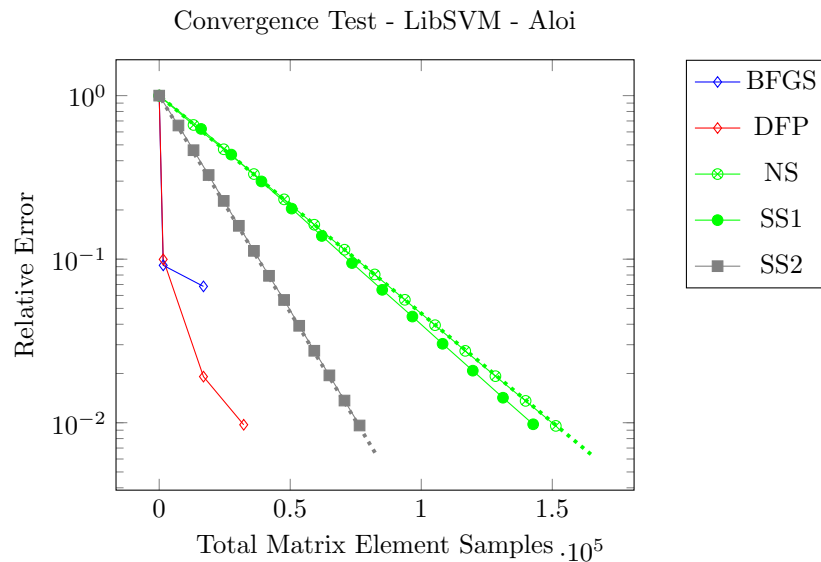


FIG. SM1. *Hessian approximation for the matrix from the LibSVM problem, Aloï ($n = 128$) [SM1] with $s = 12 = \lceil \sqrt{128} \rceil$. Dotted lines are theoretical convergence rates. Note, DFP and BFGS perform well.*

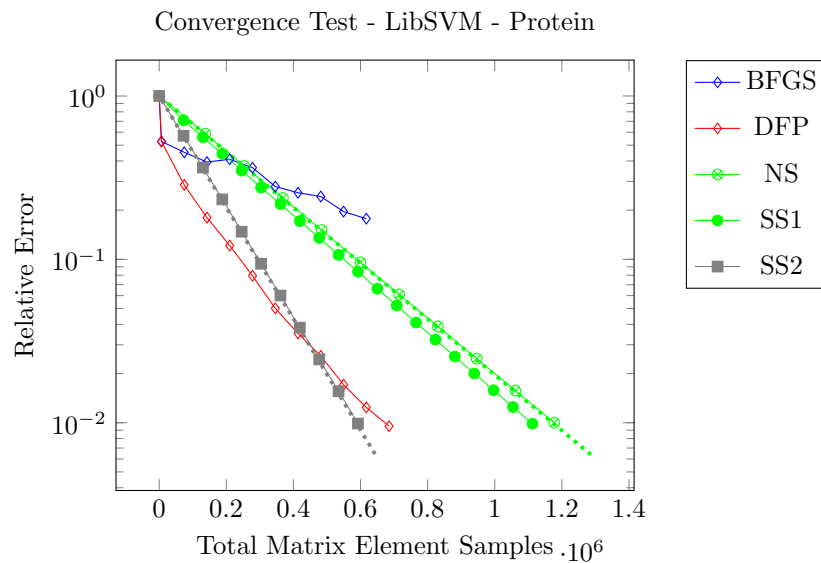


FIG. SM2. *Hessian approximation for the matrix from the LibSVM problem, Protein ($n = 357$) [SM1] with $s = 19 = \lceil \sqrt{357} \rceil$. Dotted lines are theoretical convergence rates. Note, DFP performs well, BFGS performs poorly.*

- 43 [SM1] C.-C. CHANG AND C.-J. LIN, LIBSVM: A library for support vector machines, ACM Trans-
 44 actions on Intelligent Systems and Technology, 2 (2011), pp. 27:1–27:27. Software available
 45 at <http://www.csie.ntu.edu.tw/~cjlin/libsvm>.
 46 [SM2] T. A. DAVIS AND Y. HU, The university of florida sparse matrix collection, ACM Trans. Math.
 47 Softw., 38 (2011), pp. 1:1–1:25, <https://doi.org/10.1145/2049662.2049663>, <http://doi.acm.org/10.1145/2049662.2049663>.
 48

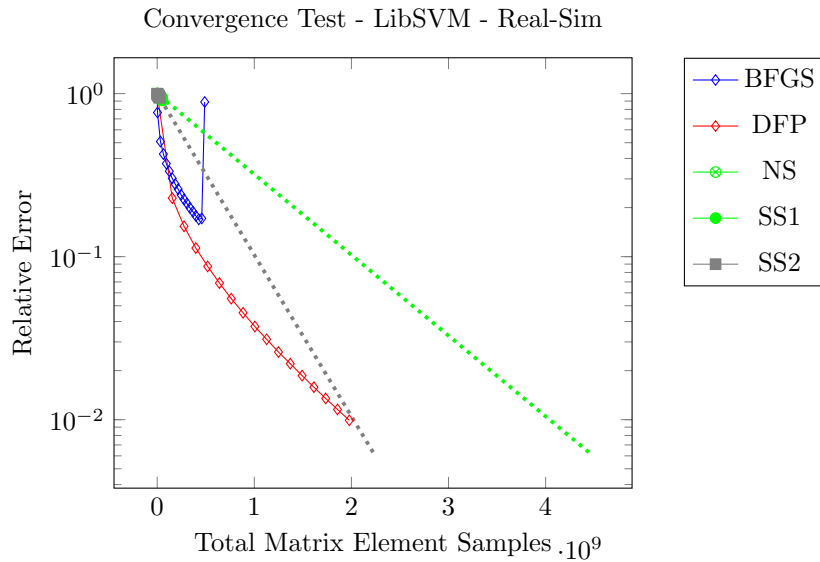


FIG. SM3. Hessian approximation for the matrix from the LibSVM problem, **Real-Sim** ($n = 20,958$) [SM1] with $s = 145 = \lceil \sqrt{20,958} \rceil$. Dotted lines are theoretical convergence rates for our algorithms. DFP performs well, BFGS does not converge.

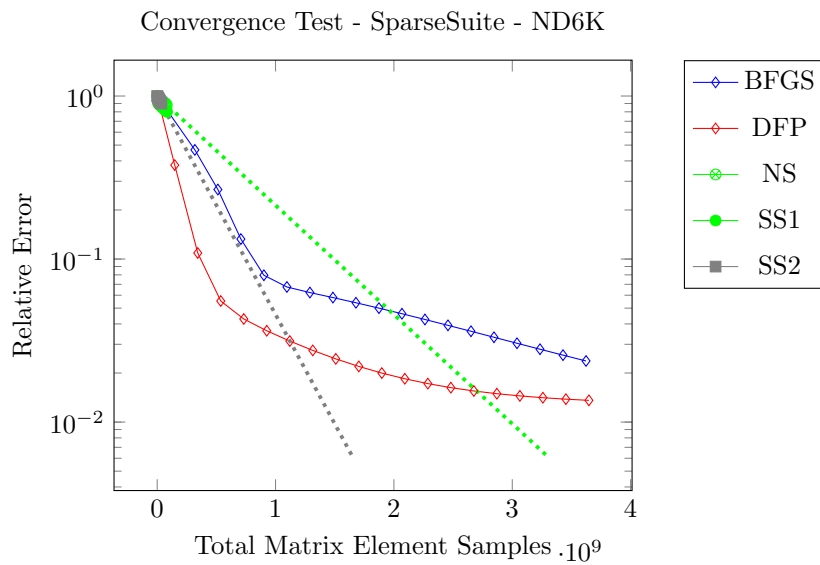


FIG. SM4. Hessian approximation for the matrix from the Sparse Suite Library, **ND6K** ($n = 18,000$) [SM2] with $s = 135 = \lceil \sqrt{18,000} \rceil$. Dotted lines are theoretical convergence rates for our algorithms.

49 [SM3] R. M. GOWER AND P. RICHÁRIK, Randomized quasi-Newton updates are linearly convergent
 50 matrix inversion algorithms, SIAM J. Matrix Anal. Appl., 38 (2017), pp. 1380–1409, <https://doi.org/10.1137/16M1062053>, <https://doi.org/10.1137/16M1062053>.
 51

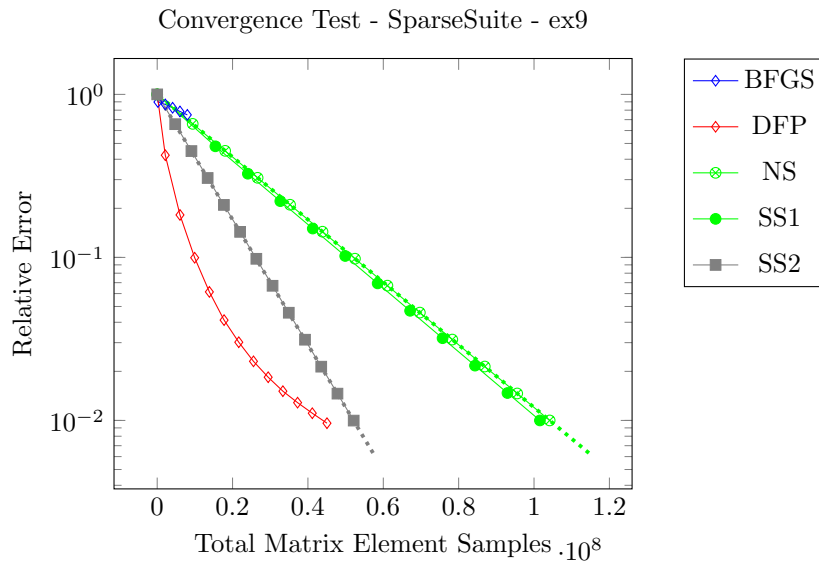


FIG. SM5. Hessian approximation for the matrix from the Sparse Suite Library, **ex9** ($n = 3363$) [SM2] with $s = 58 = \lceil \sqrt{3363} \rceil$. Dotted lines are theoretical convergence rates for our algorithms.

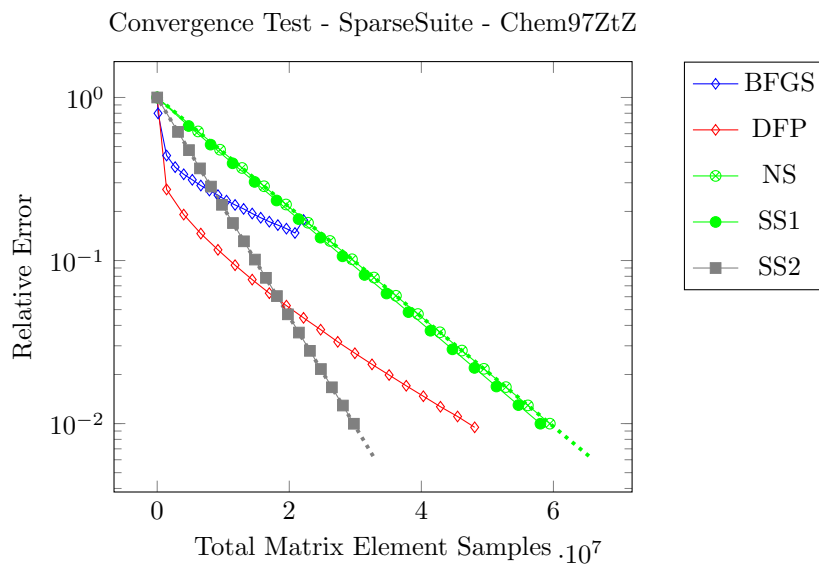


FIG. SM6. Hessian approximation for the matrix from the Sparse Suite Library, **Chem97ZtZ** ($n = 2541$) [SM2] with $s = 51 = \lceil \sqrt{2541} \rceil$. Dotted lines are theoretical convergence rates for our algorithms.

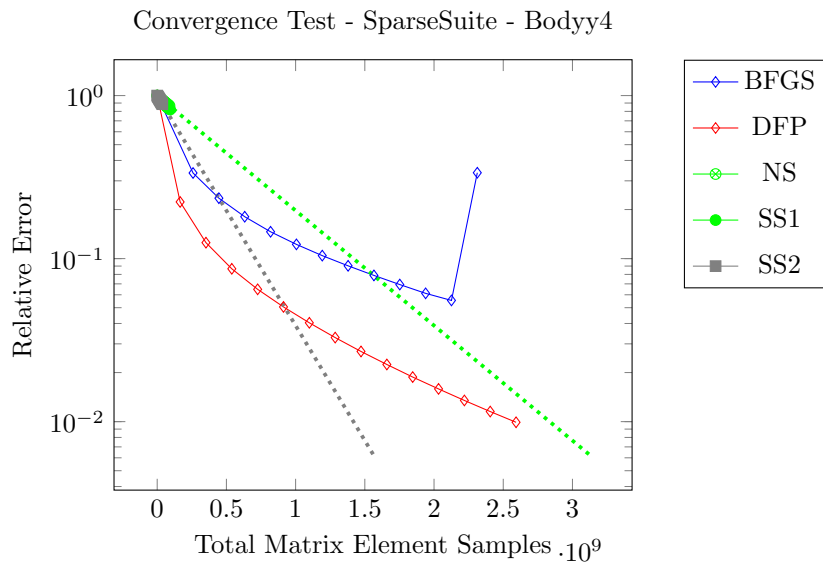


FIG. SM7. Hessian approximation for the matrix from the Sparse Suite Library, **Body** ($n = 17,546$) [SM2] with $s = 133 = \lceil \sqrt{17,546} \rceil$. Dotted lines are theoretical convergence rates for our algorithms.

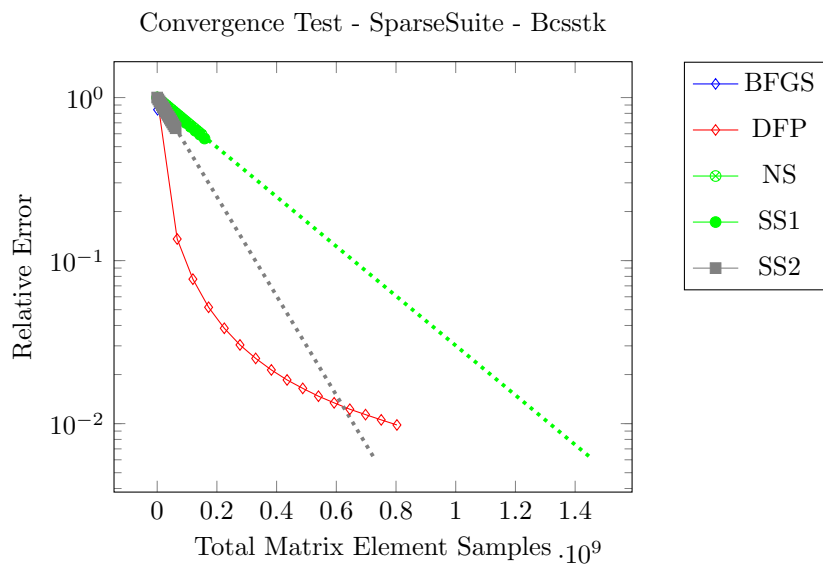


FIG. SM8. Hessian approximation for the matrix from the Sparse Suite Library, **bcsstk** ($n = 11,948$) [SM2] with $s = 110 = \lceil \sqrt{11,948} \rceil$. Dotted lines are theoretical convergence rates for our algorithms.

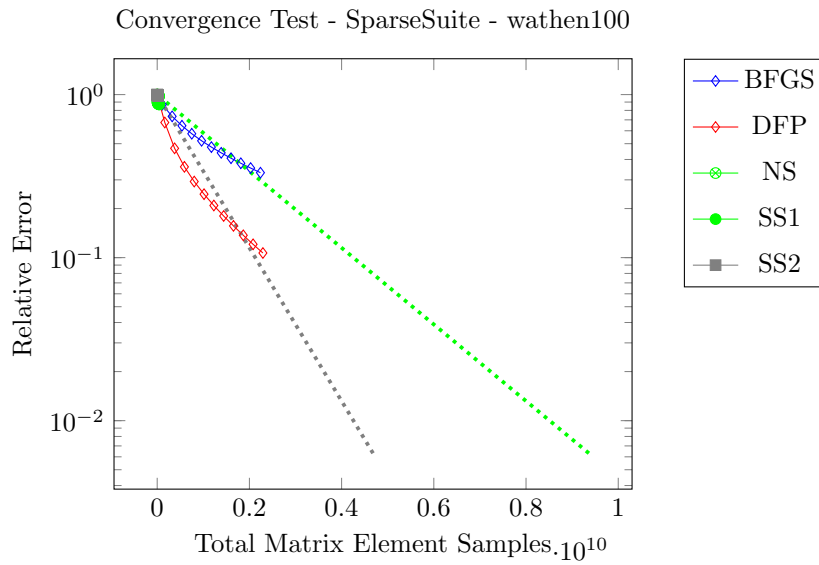


FIG. SM9. *Hessian approximation for the matrix from the Sparse Suite Library, **wathen** ($n = 30,401$) [SM2] with $s = 175 = \lceil \sqrt{30,401} \rceil$. Dotted lines are theoretical convergence rates for our algorithms.*

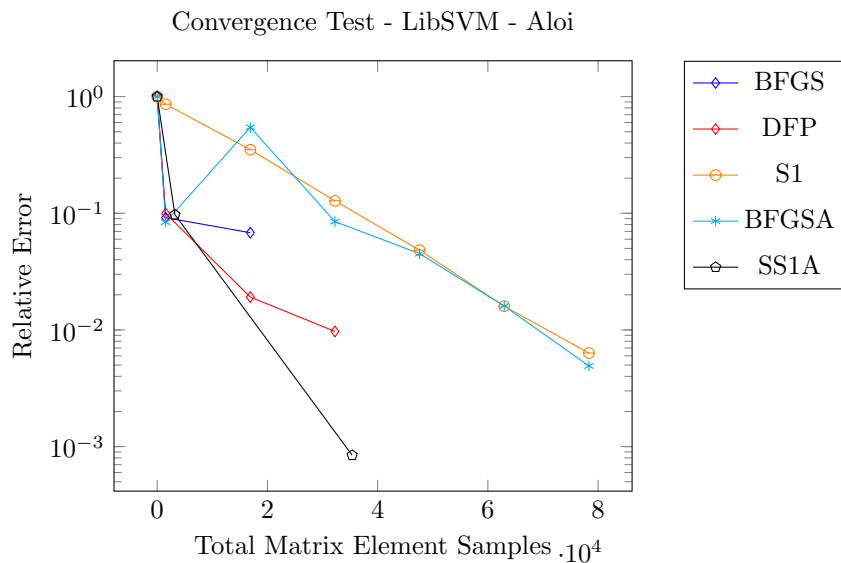


FIG. SM10. *Hessian approximation for the matrix from the LibSVM problem, **Alo1** ($n = 128$) [SM1] with $s = 12 = \lceil \sqrt{128} \rceil$.*

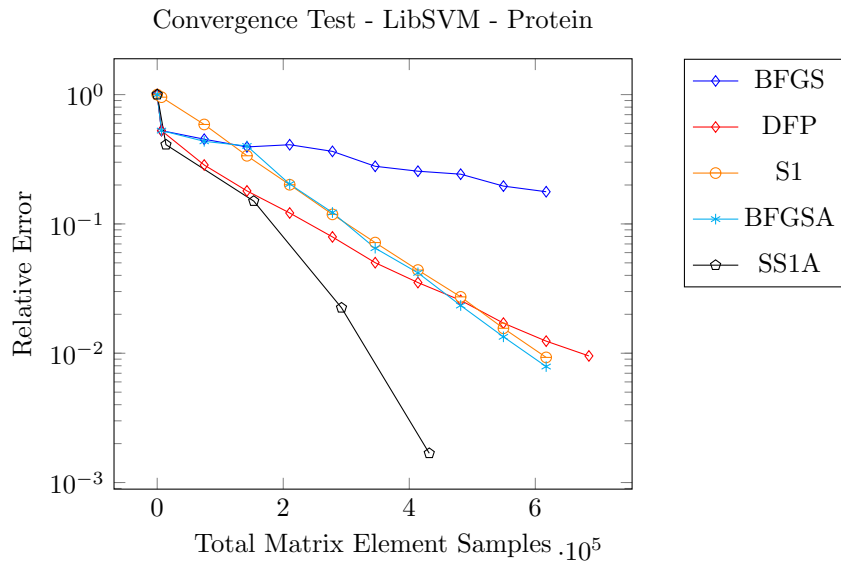


FIG. SM11. Hessian approximation for the matrix from the LibSVM problem, **Protein** ($n = 357$) [SM1] with $s = 19 = \lceil \sqrt{357} \rceil$.

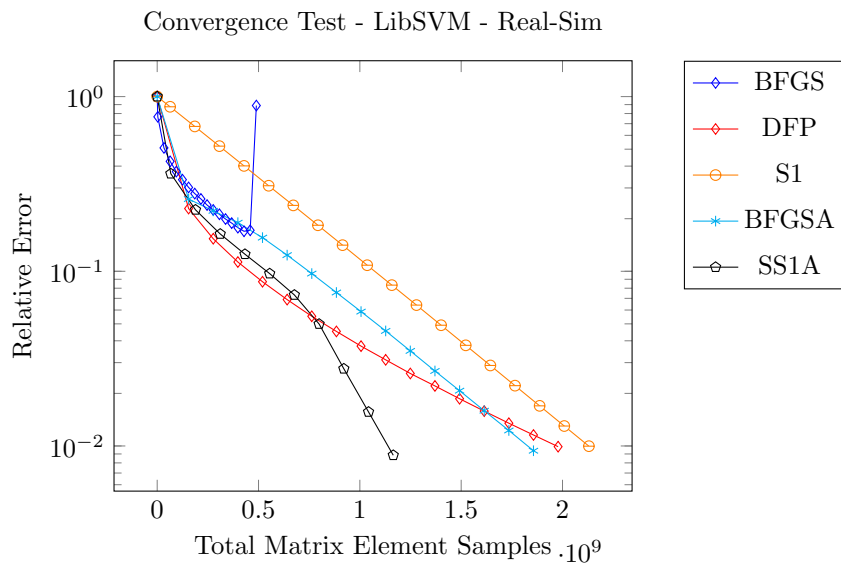


FIG. SM12. Hessian approximation for the matrix from the LibSVM problem, **Real-Sim** ($n = 20,958$) [SM1] with $s = 145 = \lceil \sqrt{20,958} \rceil$.

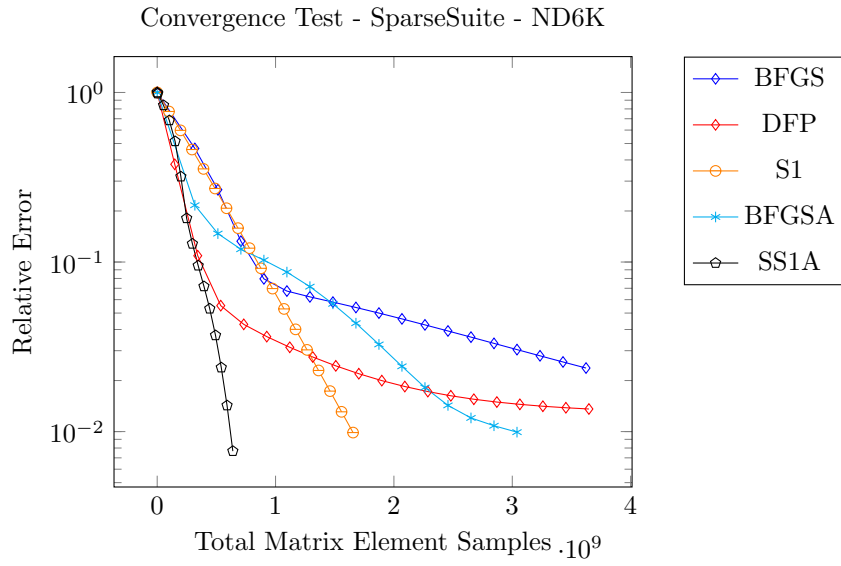


FIG. SM13. Hessian approximation for the matrix from the Sparse Suite Library, **ND6K** ($n = 18,000$) [SM2] with $s = 135 = \lceil \sqrt{18,000} \rceil$.

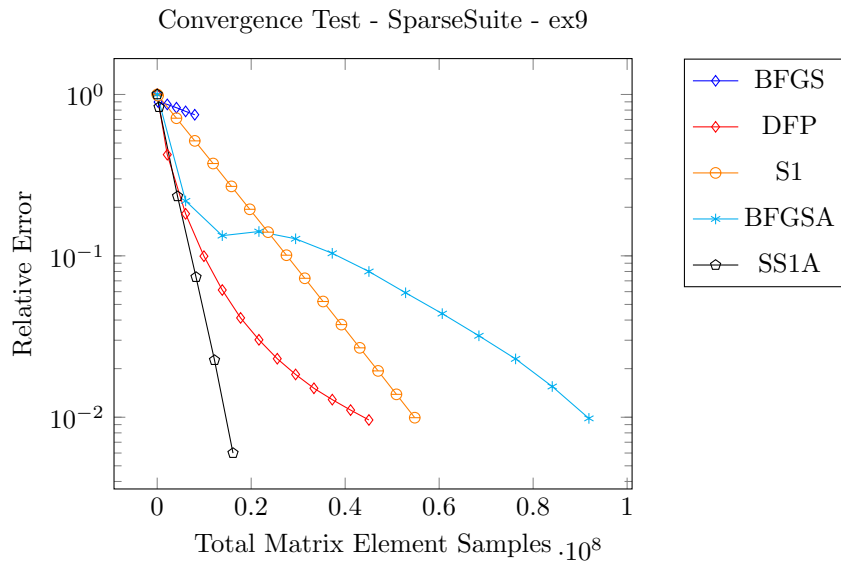


FIG. SM14. Hessian approximation for the matrix from the Sparse Suite Library, **ex9** ($n = 3363$) [SM2] with $s = 58 = \lceil \sqrt{3363} \rceil$.

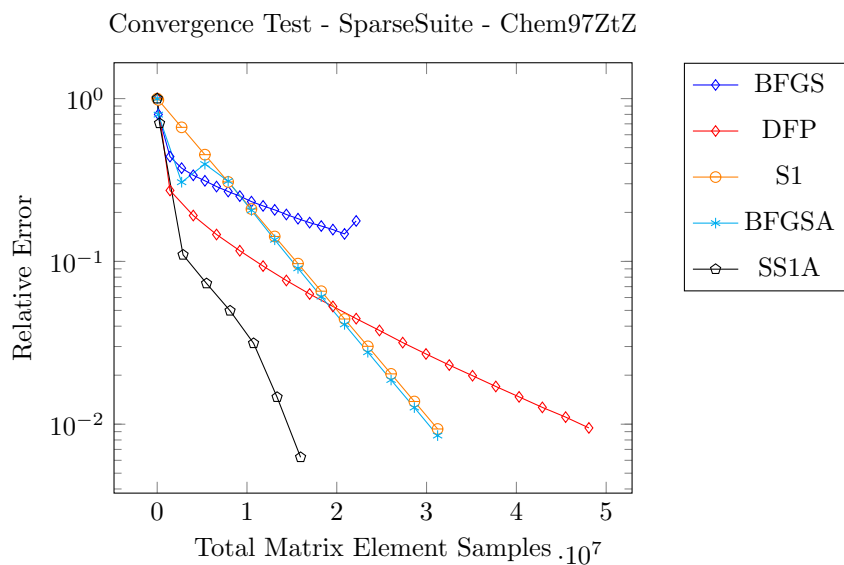


FIG. SM15. Hessian approximation for the matrix from the Sparse Suite Library, **Chem97ZtZ** ($n = 2541$) [SM2] with $s = 51 = \lceil \sqrt{2541} \rceil$.

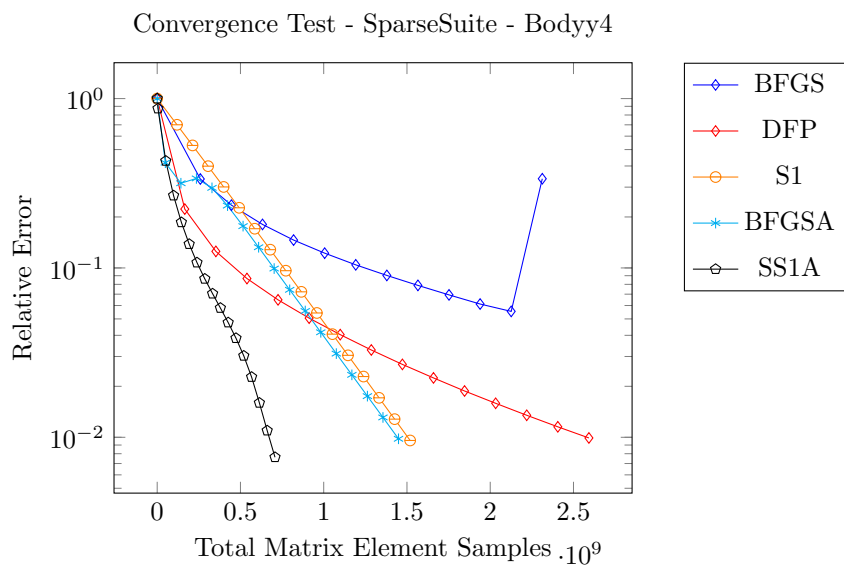


FIG. SM16. Hessian approximation for the matrix from the Sparse Suite Library, **Body** ($n = 17,546$) [SM2] with $s = 133 = \lceil \sqrt{17,546} \rceil$.

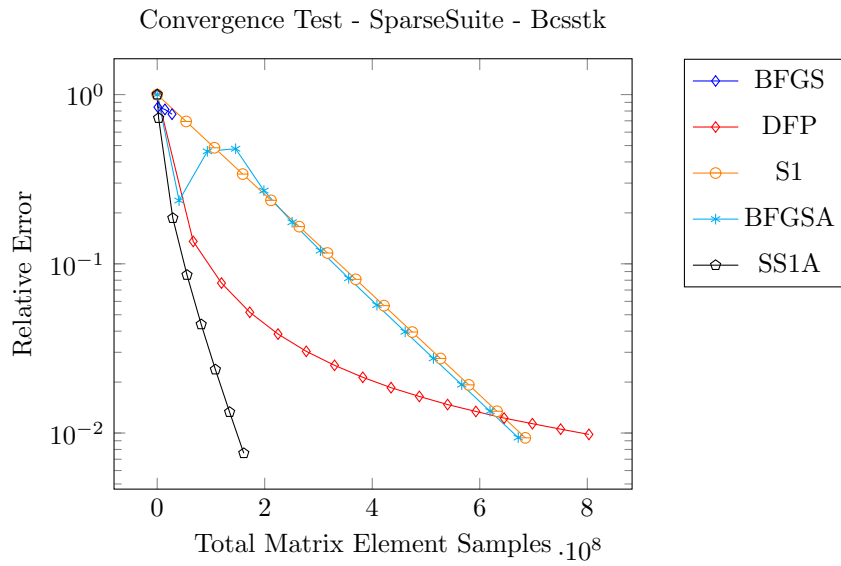


FIG. SM17. Hessian approximation for the matrix from the Sparse Suite Library, **bcsstk** ($n = 11,948$) [SM2] with $s = 110 = \lceil \sqrt{11,948} \rceil$.

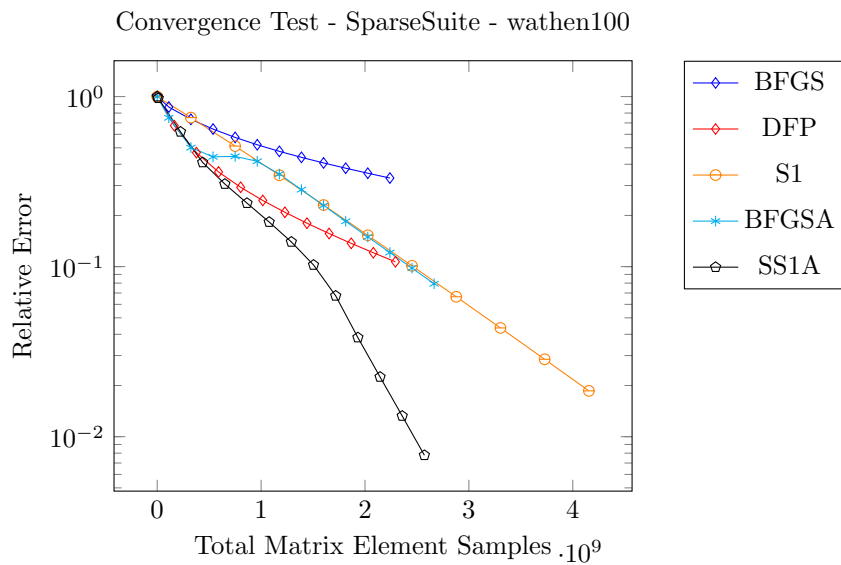


FIG. SM18. Hessian approximation for the matrix from the Sparse Suite Library, **wathen** ($n = 30,401$) [SM2] with $s = 175 = \lceil \sqrt{30,401} \rceil$.